Clim Dyn (2008) 30:391–406
DOI 10.1007/s00382-007-0296-z

# Rapid vegetation responses and feedbacks amplify climate model response to snow cover changes

**Benjamin I. Cook · Gordon B. Bonan · Samuel Levis · Howard E. Epstein**

Received: 2 April 2007 / Accepted: 17 July 2007 / Published online: 21 August 2007


**Abstract** We investigate the response of a climate system model to two different methods for estimating snow cover fraction. In the control case, snow cover fraction changes gradually with snow depth; in the alternative scenarios (one with prescribed vegetation and one with dynamic vegetation), snow cover fraction initially increases with snow depth almost twice as fast as the control method. In cases where the vegetation was fixed (prescribed), the choice of snow cover parameterization resulted in a limited model response. Increased albedo associated with the high snow caused some moderate localized cooling (3–5°C), mostly at very high latitudes (>70°N) and during the spring season. During the other seasons, however, the cooling was not very extensive. With dynamic vegetation the change is much more dramatic. The initial increases in snow cover fraction with the new parameterization lead to a large-scale southward retreat of boreal vegetation, widespread cooling, and persistent snow cover over much of the boreal region during the boreal summer. Large cold anomalies of up to 15°C cover much of northern Eurasia and North America and the cooling is geographically extensive in the northern hemisphere extratropics, especially during the spring and summer seasons. This study demonstrates the potential for dynamic vegetation within climate models to be quite sensitive to modest forcing. This highlights the importance of dynamic vegetation, both as an amplifier of feedbacks in the climate system and as an essential consideration when implementing adjustments to existing model parameters and algorithms.

**Keywords** Climate feedbacks · Snow cover · Albedo · Vegetation

B. I. Cook (✉)
Lamont Doherty Earth Observatory, Ocean and Climate Physics, 61 Route 9W, PO Box 1000, Palisades, NY 10964-8000, USA
e-mail: bc9z@ldeo.columbia.edu

G. B. Bonan · S. Levis
National Center for Atmospheric Research, 1850 Table Mesa Drive, Boulder, CO 80307-3000, USA

H. E. Epstein
Department of Environmental Sciences, University of Virginia, 291 McCormick Road, Charlottesville, VA 22903, USA

## 1 Introduction

Snow cover is an important component of the climate system, influencing the albedo and energy budget of the land surface, especially at high latitudes and in those regions with low stature vegetation (e.g., Barnett et al. 1989; Cess et al. 1991; Cohen et al. 1999). Accurate estimation of snow cover fraction is therefore crucial for realistic climate simulations (Douville et al. 1995). The portion of a given grid cell covered by snow (snow cover fraction) in climate models is typically estimated based on snow depth, although the functional relationship implemented varies widely from model to model and can lead to greatly varying estimates for snow cover and, in turn, land surface albedo. It is also fairly well established that vegetation in high latitudes can have a significant impact on land surface albedo, and albedo feedbacks to the climate system (e.g., Bonan et al. 1992). When trees are present, the relatively low albedo of the canopy can extend above the snow pack, 'masking out' the relatively high albedo of the snow beneath. If the vegetation is shorter (e.g., grasses and shrubs), the vegetation may be buried by the snow and the albedo will be higher. This provides the opportunity for strong feedbacks in the climate system associated with the

coupled snow cover/vegetation system, where a migration in the tree line (either advancing or retreating) can modulate the snow cover albedo feedback and influence the regional and global climate (Gallimore et al. 2005).

Because snow cover fraction may exert a strong influence on the base (control) climate in climate models, it is important to examine how sensitive the models may be to the estimation of this important component of the land surface. Here we investigate the impact of two different snow cover parameterizations on the climate of the Community Atmosphere Model (CAM). Because of the potentially strong influence of vegetation on land surface albedo, we consider cases with both static (prescribed) and dynamically interactive vegetation. Fully coupled models of vegetation dynamics and biogeography are becoming increasingly common within global general circulation models (e.g., Sitch et al. 2003; Krinner et al. 2005; Bonan and Levis 2006). Often they are considered part of the land surface model, despite the fact that terrestrial vegetation operates on timescales of variability and persistence often quite different from the background soil. Our study will show the potential for vegetation to be quite sensitive to relatively minor land surface climate perturbations, and demonstrate the ability of the vegetation to feedback and amplify small initial forcings into large enough perturbations to send the model climate into a new equilibrium. This occurs despite the absence of dynamical oceans or sea ice, factors previously shown to be important for amplifying vegetation feedbacks within the climate system (e.g., Brovkin et al. 2003; Claussen et al. 2006; Wohlfahrt et al. 2004). We will discuss this within the context of other studies examining high latitude vegetation feedbacks to climate and note the ramifications dynamic vegetation may have for model development.

## 2 Materials and methods

### 2.1 Model description

The atmospheric model we use is the Community Atmosphere Model, version 3 (CAM3). This model is the sixth generation of atmospheric general circulation models developed by the climate community in collaboration with the National Center for Atmospheric Research. The model features improvements to the parameterizations of moist processes, radiation processes, and aerosols (Collins et al. 2004, 2006) compared with its predecessor, CAM2. The model was run using Eulerian spectral dynamics with T42 spectral truncation (approximately 2.8° in latitude and longitude) with 26 levels in the vertical and a 20-min time step. The land model is the Community Land Model, version 3 (CLM3). This model simulates energy, moisture, and momentum fluxes between the land and atmosphere, the hydrologic cycle at the land surface, and soil temperature (Bonan et al. 2002; Oleson et al. 2004; Dickinson et al. 2006). A comprehensive discussion of the surface albedo calculations is included in Oleson et al. (2004). The snow cover parameterization is used to determine what proportion of the total ground albedo calculation is taken from the background soil albedo versus the snow albedo. Soil albedos vary by color class and whether the soils are dry or saturated. Saturated and darker soils have lower albedos. Snow albedo depends primarily upon the solar zenith angle (albedo increases above solar zenith angle of 60°). Aging effects (which would reduce albedo for older snow) are not included within this version of CLM. This could potentially lead to an overestimation of model sensitivity with the new snow cover algorithm, although the influence of this bias is likely diminished as CLM tends to underpredict snow albedo relative to observations (Peter Lawrence, personal communication). The version of CLM used in these experiments also includes substantial improvements to the land surface hydrology, including more realistic partitioning of canopy evaporation, soil evaporation, and transpiration (Lawrence et al. 2007). These improvements help reduce a dry soil bias in CLM3, leading to better simulations of photosynthesis and vegetation dynamics. Soil moisture stress on transpiration and photosynthesis is reduced and interseasonal water storage is increased, allowing plants to maintain higher rates of transpiration and photosynthesis throughout the dry season. Relative to other coupled models, CAM3-CLM3 exhibits some of the strongest land–atmosphere coupling (Guo et al. 2006; Koster et al. 2006), particularly during the boreal summer (June–July–August). Land surface forcing of climate may therefore be stronger within this model, relative to others.

CLM3 operates on the same spatial grid as CAM3. Figure 1 compares results from a control run of CAM3 and CLM3 with fixed vegetation (solid lines) and observations (dashed lines) (Foster and Davy 1988; Willmott and Matsura 2000; Fekete et al. 2000, 2002). Shown are climatological seasonal cycles in 2-m air temperature, precipitation, runoff, and snow depth for each hemisphere. Overall, the model does a reasonable job reproducing the observed climate. In the northern hemisphere the model tends to slightly over estimate temperature, precipitation, and snow depth, although the seasonal cycles are well resolved. Similar results are seen in the southern hemisphere, except for a gross overestimation of snow depth. The overestimation occurs primarily over Antarctica where, even in our control run, the snow cover over this region approaches 1.0 and varies little throughout the year. This region also lacks any significant vegetation cover. These factors make it unlikely that our new snow cover parameterization will cause a significant model response

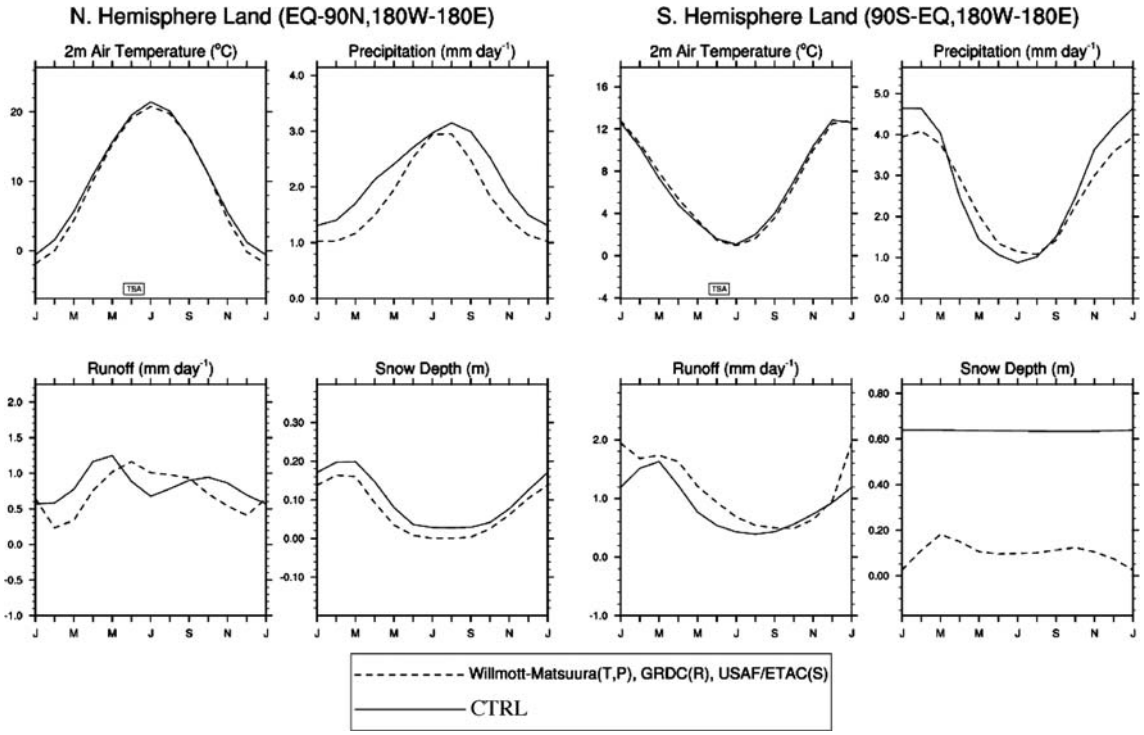


**Fig. 1** Monthly observed climatologies for selected surface variables (2-m air temperature, precipitation, runoff, snow depth), compared to CTRL, our fixed vegetation control run using original CLM3 snow cover

over Antarctica, and also suggests there is little capacity for vegetation feedbacks to amplify the model response over this region. For this study, we focus our analyses on the extratropical northern hemisphere response, where feedbacks between snow cover and vegetation are likely to be most important.

The dynamic vegetation model, CLM-DGVM, is a plant functional type (PFT) model based on the Lund-Potsdam-Jena (LPJ)-DGVM (Sitch et al. 2003; Bonan and Levis 2006). Figure 2 compares selected plant functional type distributions from a long (>400 years) unforced run of the CAM3-CLM3 against satellite observations. By unforced, we mean that the model was allowed to run with no external forcings, such as increasing atmospheric carbon dioxide. Long integrations such as these are used to come up with a base model climate used as the reference 'control' case when comparing model runs. The model places the PFTs in the correct geographical locations, although both tree and grass PFT distributions tend to be overestimated compared to observations. This is largely due to the fact that this version of CLM-DGVM does not include shrub or crop PFTs that are contained in the observational dataset.

## 2.2 Snow cover fraction parameterizations

The relationships between snow cover fraction and snow depth for two different parameterizations are shown in Fig. 3. The dashed curve with filled circles is the default relationship in CLM3 (Oleson et al. 2004), where fractional snow cover initially increases relatively rapidly with snow depth (fractional coverage equal to 0.50 at snow depths of 0.10 m) and then slowly saturates. Even at snow depths of 1 m, the fractional coverage is still only about 0.90. In sharp contrast is the function developed by Yang et al. (1997) and evaluated in the Biosphere Atmosphere Transfer Scheme (BATS) (hereafter referred to as "Y97"). Here, at a depth of 0.10 m, snow cover fraction is 0.96, which is much greater than for the default case. The original calculation in BATS was very similar to the current CLM3 relationship, but this new function was found to give better agreement between model estimates and observations for both snow cover and surface albedo, within BATS (Yang et al. 1997). Our goal here is not necessarily model improvement, but to examine the sensitivity of the model to the choice of snow cover parameterization.

## 2.3 Experimental setup

All simulations were run with climatologically fixed sea surface temperatures and sea ice distributions and started from identical initial conditions, including vegetation distributions. Our goal was to focus solely on the potential amplifying effect of dynamic vegetation. The three cases

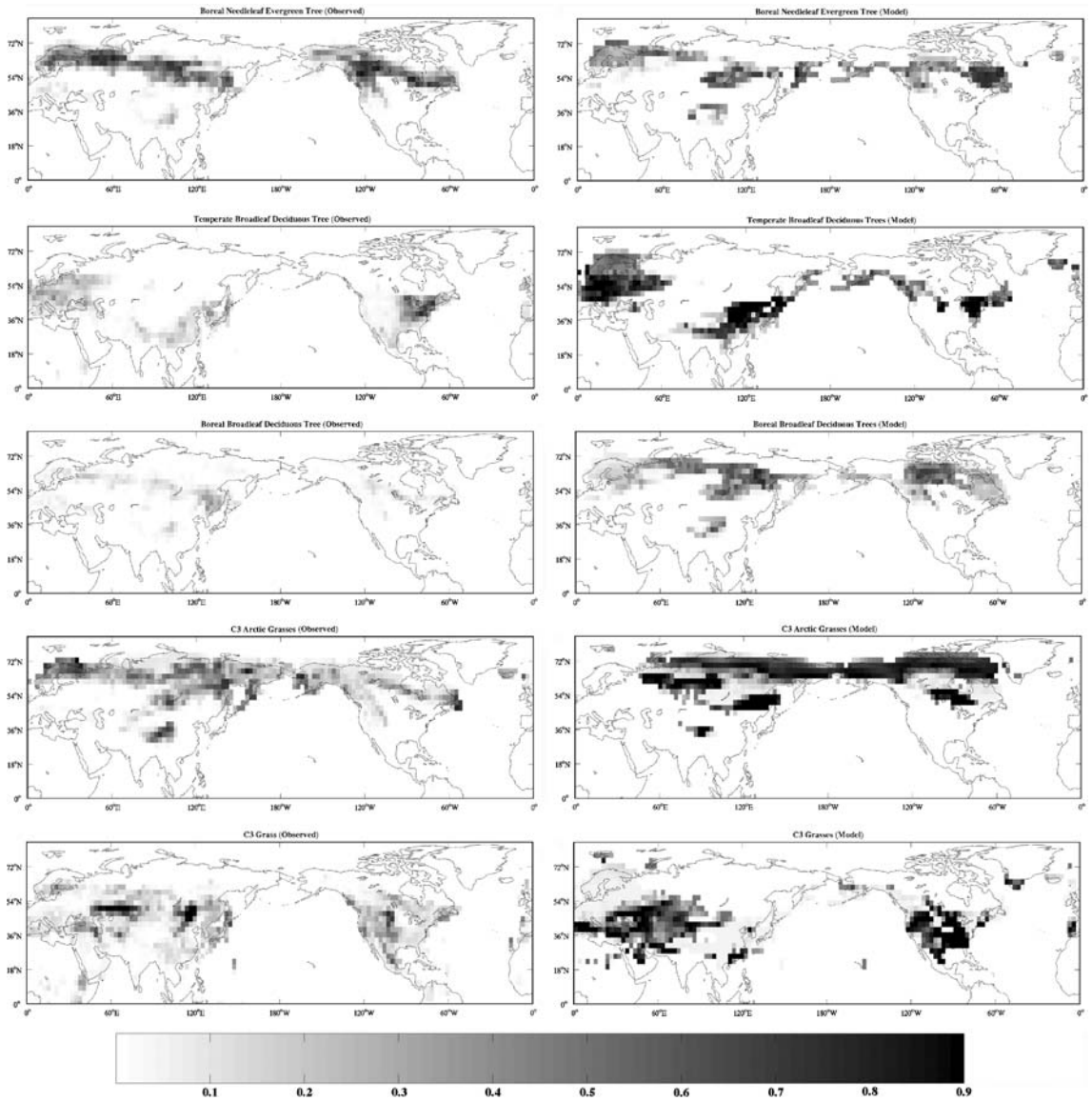


**Fig. 2** Comparison of selected observed boreal plant functional type distributions with modeled distributions from a long control run of CAM3-CLM3 with dynamic vegetation

run and analyzed were (1) fixed vegetation and CLM snow cover (CTRL), (2) fixed vegetation and Y97 snow cover (FV-Y97), and (3) dynamic vegetation and Y97 snow cover (DV-Y97). Vegetation distributions were taken from a long, unforced, coupled control run of CAM3 and CLM3 with dynamic vegetation; these distributions are used as the initial vegetation in DV-Y97 and as the prescribed vegetation in CTRL and FV-Y97. Because our initial vegetation distributions for our CTRL run were taken from these model predicted distributions, our fixed vegetation CTRL run is analogous to a DV-CTRL run. CTRL can thus be used as the standard for comparison against the fixed vegetation (FV-Y97) and the dynamic vegetation (DV-Y97) scenarios. Fixed vegetation model runs (CTRL and FV-Y97) were 31 years long; the first 10 years were used as "spin up" and the subsequent 21 years were averaged and used for analysis. Ten years should be enough time for spin up because climate system memory at the land surface is relatively short (on the order of months and several years) compared to other components of the climate system (decades and centuries; e.g., in ocean temperatures). Time series plots of selected land surface variables (soil temperature, 2-m air temperature etc., not shown) indicate no trends after the 10-year spin-up. The timescales of response

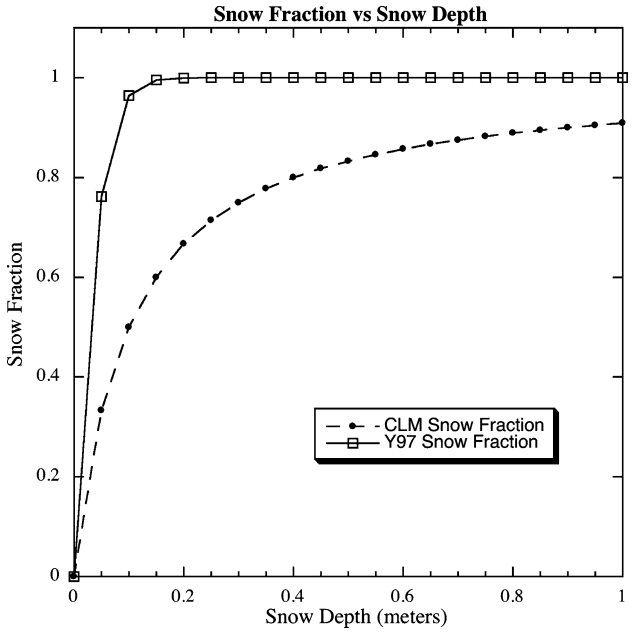


**Fig. 3** Parameterizations for determining snow cover from snow depth: Y97 (*solid line*, *open squares*) and CLM3 (*dashed line*, *solid circles*)

for vegetation dynamics are on the order of years, and thus model runs with dynamic vegetation require longer spin up and integration times. The DV-Y97 run was 100 years long; the first 79 years were used as "spin up" and the subsequent 21 years were averaged and used for analysis. Vegetation changes during the last 20 years were minor, relative to the spin up period.

## 3 Results

### 3.1 Snow cover and albedo

The Y97 snow algorithm increased the snow-covered area in both the static and dynamic vegetation scenarios. Table 1 shows these changes, broken down by season and latitude band, in units of $10^5$ km$^2$. Greatest increases are seen in the transition seasons (MAM and SON), for latitude bands 50°N–80°N. During JJA, there are also large increases in snow-covered area north of 60°N, especially in DV-Y97. The new snow cover parameterization led to substantial increases in surface albedo over much of the northern hemisphere, as shown in the first set of difference plots (Figs. 4, 5, 6) comparing FV-Y97 minus CTRL (Fig. 4), DV-Y97 minus CTRL (Fig. 5), and DV-Y97 minus FV-Y97 (Fig. 6). Statistically significant differences were assessed using a two-sided Students *t* test; statistically insignificant differences ($P > 0.05$) have been masked out. Albedo anomalies in the fixed vegetation scenario (Fig. 4) are uniformly positive and modest in magnitude, driven solely by the increased snow cover and rarely exceeding +0.20. When dynamic vegetation is included (Figs. 5, 6), the albedo anomalies cover a much wider geographic area and are much higher compared to the fixed vegetation scenario, in some cases exceeding +0.60. Additionally, several areas show some minor decreases in albedo, on the order of −0.10. These albedo differences in DV-Y97 are due to changes in the distribution of plant functional types (Table 2). In most areas, the vegetation retreated southward, exposing more of the snow surface and leading to higher albedos. In the few regions where certain plant functional types actually expanded, there were slight decreases in albedo. This dynamic vegetation response will be revisited and explained in greater detail later.

### 3.2 Temperature response

To assess the climate response of the model we compare the 2-m air temperature over land between runs: FV-Y97 minus CTRL (Fig. 7), DV-Y97 minus CTRL (Fig. 8), and DV-Y97 minus FV-Y97 (Fig. 9). As in previous difference plots, significant differences for Figs. 7, 8 and 9 were assessed using a two-sided Students *t* test; insignificant differences ($P > 0.05$) have been masked out.

In the FV-Y97 scenarios, the spatial extent of the cold temperature anomalies is limited and of moderate magnitude (Fig. 7). Peak cooling anomalies occur over the Tibetan plateau in winter and spring (DJF and MAM), with changes on the order of 3–5°C. The rest of the extra-tropics rarely cool more than 1–2°C during DJF and MAM, or 0.5°C during JJA and SON. When dynamic vegetation is included, the initially small model response to the Y97 snow cover becomes amplified (Figs. 8, 9). With the initial cooling anomaly, the boreal vegetation begins to retreat, manifested largely as a reduction in the extent of boreal needleleaf evergreen trees and boreal broadleaf deciduous trees (Table 2). What accounts for the changes in these (and other) vegetation distributions? Within the CLM-DGVM, vegetation mortality, survival, and establishment are driven by two factors: net primary productivity (NPP, i.e., plant net carbon balance) and bioclimatic thresholds (Levis et al. 2004). The NPP calculation is ultimately a function of climate (e.g., temperature, water availability, etc.) and mortality of plant functional types occurs when NPP is negative. Survival and establishment are based on bioclimatic thresholds-specifically, 20 year running means of coldest minimum monthly temperature ($T_{c,min}$), warmest minimum monthly temperature ($T_{c,max}$), and minimum annual growing degree days above 5°C ($GDD_{min}$). The different plant functional types are largely distinguished by different bioclimatic limits. For example, a temperate

**Table 1** Snow covered area, by latitude and season, in units of $10^5$ km$^2$, for each model scenario

| Latitude band | CTRL | FV-Y97 | DV-Y97 | Difference FV-CTRL | Difference DV-CTRL |
|---|---|---|---|---|---|
| Snow covered area ($10^5$ km$^2$): DJF | | | | | |
| 80°N–90°N | 4.58 | 5.18 | 5.18 | 0.60 | 0.60 |
| 70°N–80°N | 63.06 | 75.97 | 76.05 | 12.91 | 12.99 |
| 60°N–70°N | 106.23 | 132.33 | 132.66 | 26.10 | 26.43 |
| 50°N–60°N | 118.21 | 166.82 | 166.88 | 48.61 | 48.67 |
| 40°N–50°N | 51.64 | 111.12 | 113.64 | 59.48 | 62.00 |
| 30°N–40°N | 19.81 | 33.70 | 35.52 | 13.89 | 15.71 |
| Snow covered area ($10^5$ km$^2$): JJA | | | | | |
| 80°N–90°N | 3.50 | 5.18 | 5.18 | 1.68 | 1.68 |
| 70°N–80°N | 24.66 | 46.28 | 67.94 | 21.62 | 43.29 |
| 60°N–70°N | 7.85 | 16.13 | 55.90 | 8.28 | 48.06 |
| 50°N–60°N | 0.12 | 0.53 | 6.73 | 0.40 | 6.60 |
| 40°N–50°N | 0.00 | 0.00 | 0.10 | 0.00 | 0.09 |
| 30°N–40°N | 0.23 | 1.50 | 6.02 | 1.26 | 5.79 |
| Snow covered area ($10^5$ km$^2$): MAM | | | | | |
| 80°N–90°N | 4.65 | 5.18 | 5.18 | 0.53 | 0.53 |
| 70°N–80°N | 63.45 | 75.20 | 75.30 | 11.75 | 11.84 |
| 60°N–70°N | 90.85 | 116.74 | 121.41 | 25.90 | 30.57 |
| 50°N–60°N | 67.11 | 101.70 | 116.61 | 34.59 | 49.50 |
| 40°N–50°N | 14.05 | 36.88 | 55.89 | 22.83 | 41.84 |
| 30°N–40°N | 11.59 | 19.45 | 23.14 | 7.86 | 11.55 |
| Snow covered area ($10^5$ km$^2$): SON | | | | | |
| 80°N–90°N | 4.19 | 5.18 | 5.18 | 0.99 | 0.99 |
| 70°N–80°N | 41.66 | 61.77 | 68.99 | 20.11 | 27.33 |
| 60°N–70°N | 42.83 | 73.80 | 81.55 | 30.97 | 38.72 |
| 50°N–60°N | 21.99 | 48.39 | 50.85 | 26.40 | 28.86 |
| 40°N–50°N | 4.11 | 13.69 | 14.36 | 9.58 | 10.24 |
| 30°N–40°N | 3.82 | 9.34 | 10.82 | 5.51 | 7.00 |

broadleaf deciduous tree requires warmer temperatures and a longer growing season to survive and establish ($T_{c,min}$ = 17°C, $T_{c,max}$ = 15.5°C, $GDD_{min}$ = 1,200) than a boreal needleleaf evergreen tree ($T_{c,min}$ = −32.5°C, $T_{c,max}$ = 2.0°C, $GDD_{min}$ = 600). The fact that these parameters are based on 20 year running means ensures that only a persistent change in climate can cause shifts in vegetation distributions. The vegetation response seen in scenario DV-Y97, then, is ultimately a response to the changing climate—a colder equilibrium that favors certain functional types over others. Combined, losses of boreal needleleaf evergreen trees and boreal broadleaf deciduous trees amounted to a ~2.7 million km$^2$ reduction in forest cover above 50°N, replaced partially by C3 arctic grasses near the 50°N baseline. Normally, these tall trees would 'mask out' any snow below the canopy, keeping a relatively low albedo despite the increases in snow cover fraction. As the trees die off and the treeline moves south, this masking effect is removed, and more of the snow surface is exposed. Because of this we see higher anomalous albedo values and cooler temperatures in the dynamic compared to the fixed vegetation scenarios. The initially minor cooling from the expanded snow cover leads to a vegetation dieback, leading to even higher surface albedos, more cooling, and a self-reinforcing feedback loop that leads the climate to a new, much colder equilibrium climate. Changes are most severe during JJA (~15°C in some areas), where cooler temperatures lead to persistent snow cover (and higher albedos) throughout the season, especially over Eurasia. Also notable is an area of warming in northwest North America during DJF. These warm anomalies are related to changes in low level winds and dynamics, leading to advection from the relatively warmer oceans onto the cooler continents. The warm anomaly in northwest North America is specifically related to an intensification of the Aleutian low. Some regions see a slight decrease in albedo, of about 0.10 (Fig. 5). These were areas initially too warm for boreal trees in the CTRL simulation. The cooling in DV-

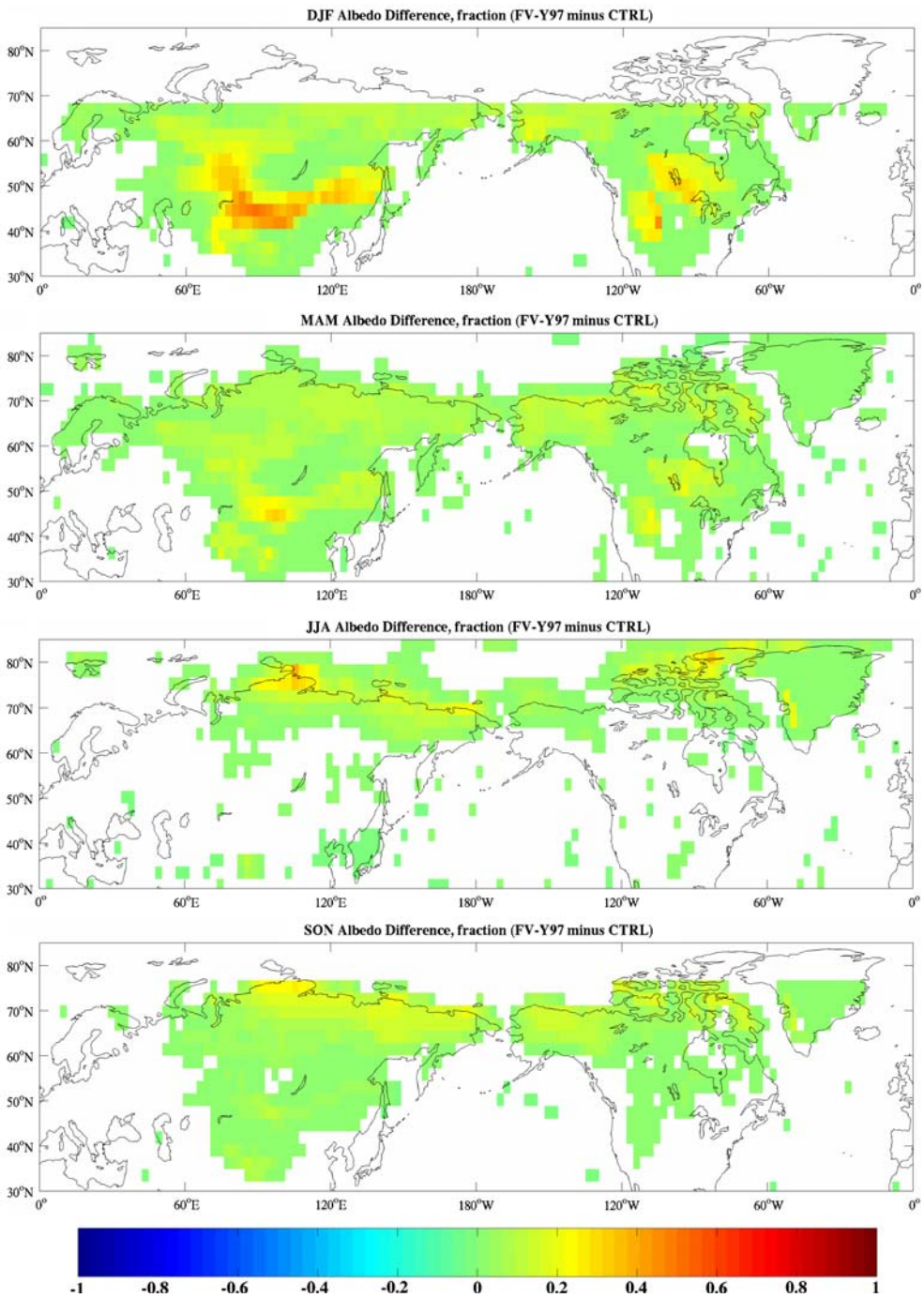


**Fig. 4** Difference in surface ALBEDO for all four seasons between the fixed vegetation case and control run (FV-Y97 minus CTRL). Insignificant differences have been masked out

Y97 led to temperatures too cool for the existence of trees in the northern part of the continents but, in these other regions, the cooling allowed for expansion of boreal, relative to temperate trees, specifically boreal needleleaf evergreen trees and boreal broadleaf deciduous trees. This led to slightly lower albedos, especially during the winter and spring seasons, and increased radiation absorption at the surface, although this increased absorption was not enough to counter the larger scale cooling.

The main forcing for the changes in both scenarios (fixed and dynamic vegetation) is the increased albedo (Figs. 4, 5, 6) from the increased snow cover. This can be confirmed through examination of the surface energy balance (Table 3). Here we break up the analysis by season and latitude, looking at the high latitudes (60°N–90°N) and the midlatitudes (30°N–60°N) separately. In most cases and seasons, both the fixed and dynamic vegetation scenarios show large reductions in absorbed radiation and

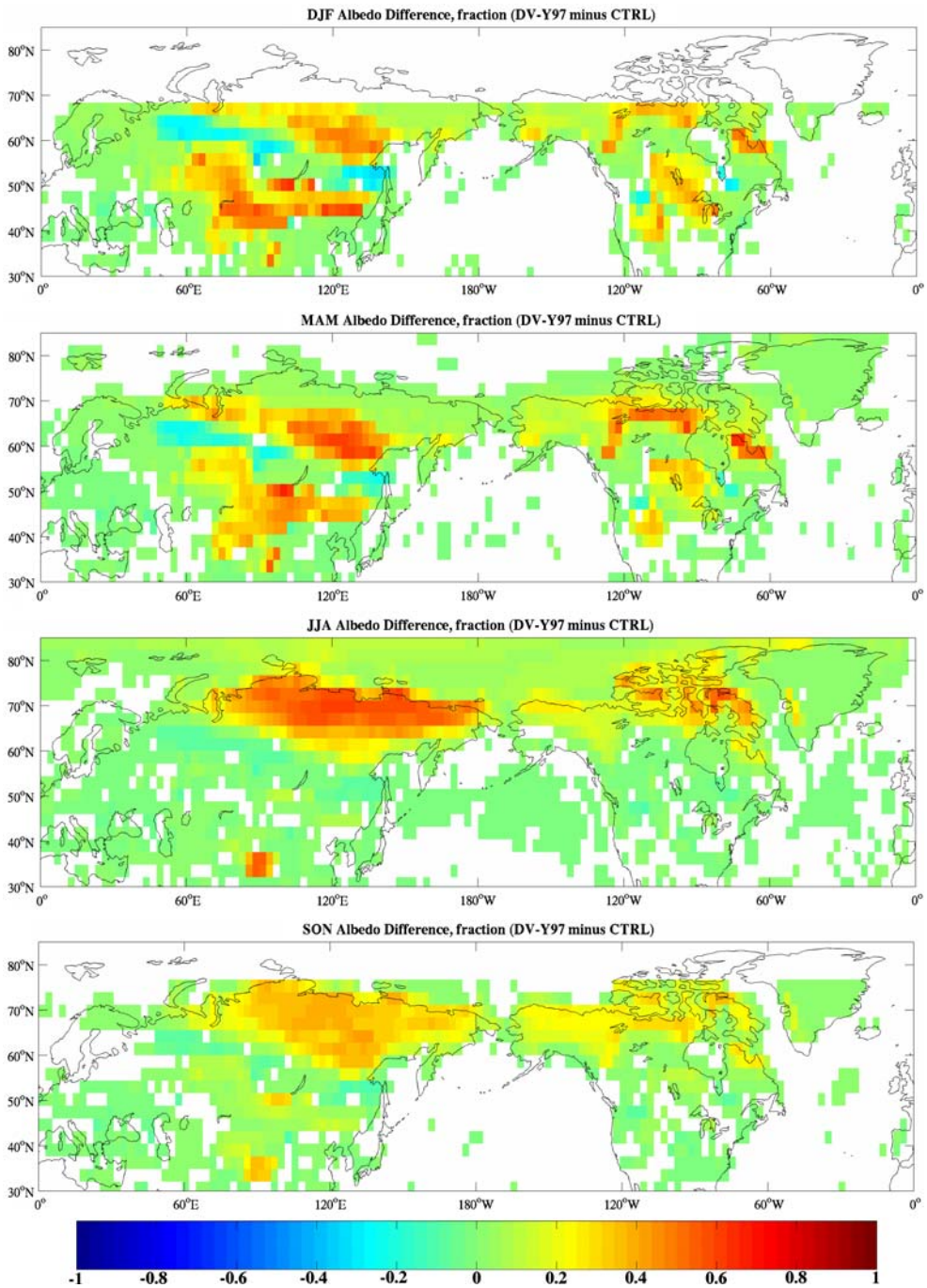


**Fig. 5** Difference in surface ALBEDO for all four seasons between the dynamic vegetation case and control run (DV-Y97 minus CTRL). Insignificant differences have been masked out

increases in reflected radiation. The amplifying effect of the dynamic vegetation is such that these variables increase greatly when DV-Y97 is compared to FV-Y97. An alternative hypothesis for the cooling during summer could be a delayed snow melt, wetter soils, and greater latent relative to sensible heating. However, the energy balance shows that, in general, both latent and sensible heating across seasons and latitudes decreases. Additionally, the magnitude of these anomalies is quite small, relative to the changes in reflected and absorbed radiation, again reinforcing the albedo related cooling as the predominant factor.

## 4 Discussion

The work here highlights two main points related to the role of snow cover in the climate system and climate

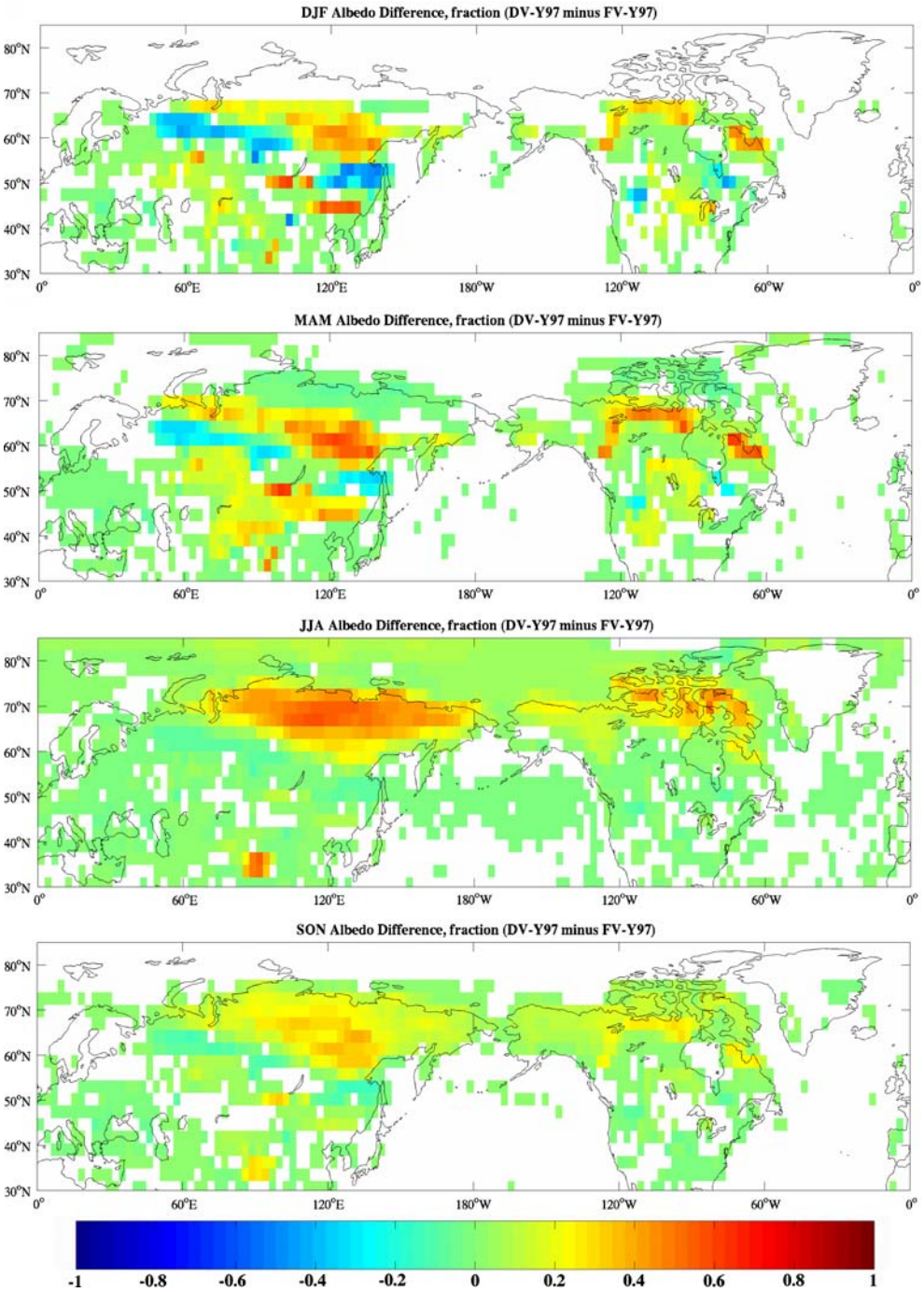


**Fig. 6** Difference in surface ALBEDO for all four seasons between the dynamic vegetation case and fixed vegetation case (DV-Y97 minus FV-Y97). Insignificant differences have been masked out

models. First it emphasizes, much like previous studies (e.g., Bonan et al. 1992; Ganopolski et al. 1998; Gallimore et al. 2005; Levis et al. 1999), the important role that terrestrial vegetation plays in amplifying albedo feedbacks related to snow cover. The novelty of our study lies in both the response of the vegetation and the magnitude of the subsequent feedback. When the static vegetation scenarios (FV-Y97 and CTRL) are compared, the albedo and temperature anomalies are small and highly localized. These small perturbations, however, are enough to initiate a retreat of high latitude vegetation in DV-Y97. With the initial retreat, the vegetation feedback is strong enough to continue to exacerbate the temperature and albedo anomalies, resulting in further vegetation changes and eventually a new, much colder equilibrium climate. These vegetation and climate changes happen rapidly, with the climate and vegetation reaching a new equilibrium after only a few decades. This occurs despite the absence of interactive

**Table 2** Changes in areal extent ($km^2$) of selected boreal plant functional types in the DV-Y97 scenario, broken down by PFT and latitude band

| Latitude band | Initial | Mean (80–100 years) | Difference |
|---|---|---|---|
| PFT covered area ($km^2$): boreal needleaf evergreen tree | | | |
| **80°N–90°N** | **1** | **0** | **−1** |
| **70°N–80°N** | **107,020** | **92,257** | **−14,763** |
| **60°N–70°N** | **1,294,500** | **992,534** | **−301,966** |
| **50°N–60°N** | **5,012,900** | **4,612,838** | **−400,062** |
| 40°N–50°N | 1,007,000 | 1,254,676 | 247,676 |
| 30°N–40°N | 630,750 | 696,074 | 65,324 |
| PFT covered area ($km^2$): temperate broadleaf deciduous tree | | | |
| 80°N–90°N | 0 | 0 | 0 |
| 70°N–80°N | **51,259** | **50,931** | **−328** |
| **60°N–70°N** | **1,057,200** | **1,047,724** | **−9,476** |
| **50°N–60°N** | **4,900,900** | **4,503,857** | **−397,043** |
| **40°N–50°N** | **6,104,400** | **5,673,062** | **−431,338** |
| 30°N–40°N | 2,607,900 | 2,761,790 | 153,890 |
| PFT covered area ($km^2$): boreal broadleaf deciduous tree | | | |
| 80°N–90°N | **3** | **0** | **−3** |
| **70°N–80°N** | **18,451** | **16,026** | **−2,425** |
| **60°N–70°N** | **2,507,800** | **834,833** | **−1,672,967** |
| **50°N–60°N** | **3,726,200** | **3,386,229** | **−339,971** |
| 40°N–50°N | 517,700 | 773,243 | 255,543 |
| **30°N–40°N** | **421,280** | **184,320** | **−236,960** |
| PFT covered area ($km^2$): C3 arctic grass | | | |
| **80°N–90°N** | **353** | **203** | **−150** |
| **70°N–80°N** | **1,659,100** | **41,806** | **−1,617,294** |
| **60°N–70°N** | **6,511,000** | **1,755,938** | **−4,755,062** |
| 50°N–60°N | 4,445,400 | 4,648,976 | 203,576 |
| 40°N–50°N | 2,109,200 | 2,610,414 | 501,214 |
| **30°N–40°N** | **559,420** | **265,410** | **−294,010** |
| PFT covered area ($km^2$): C3 grass | | | |
| 80°N–90°N | 0 | 0 | 0 |
| **70°N–80°N** | **143,860** | **87,545** | **−56,315** |
| **60°N–70°N** | **341,470** | **253,694** | **−87,776** |
| **50°N–60°N** | **1,475,100** | **1,436,571** | **−38,529** |
| **40°N–50°N** | **7,898,300** | **5,899,971** | **−1,998,329** |
| **30°N–40°N** | **6,858,000** | **6,242,748** | **−615,252** |

The difference is between the initial vegetation distribution and average distributions for the last 20 years of the DV-Y97 simulation. Bold values indicate the negative changes

ocean or sea ice dynamics, factors in previous studies that have been show to be important for amplifying vegetation feedbacks to climate (e.g., Brovkin et al. 2003; Claussen et al. 2006; Wohlfahrt et al. 2004). Our results suggest vegetation dynamics alone may be large enough to significantly alter the model climate, even in the absence of other amplifying factors. This also suggests that feedbacks in the coupled vegetation–climate system may be more sensitive to equilibrium transitions than suggested in other modeling work. Brovkin et al. (2003), for example, found that vegetation feedbacks in the high latitudes were not strong enough to support multiple steady states in both present day (similar to our study) and doubled $CO_2$ climates. This contrasts markedly with our study, where we have demonstrated that it may only take a slight push to send the entire system into a new equilibrium.

Secondly, the response of the vegetation speaks directly to model development and sensitivity testing. If the Y97 algorithm were integrated into the model and tested without considering dynamic vegetation, one might conclude

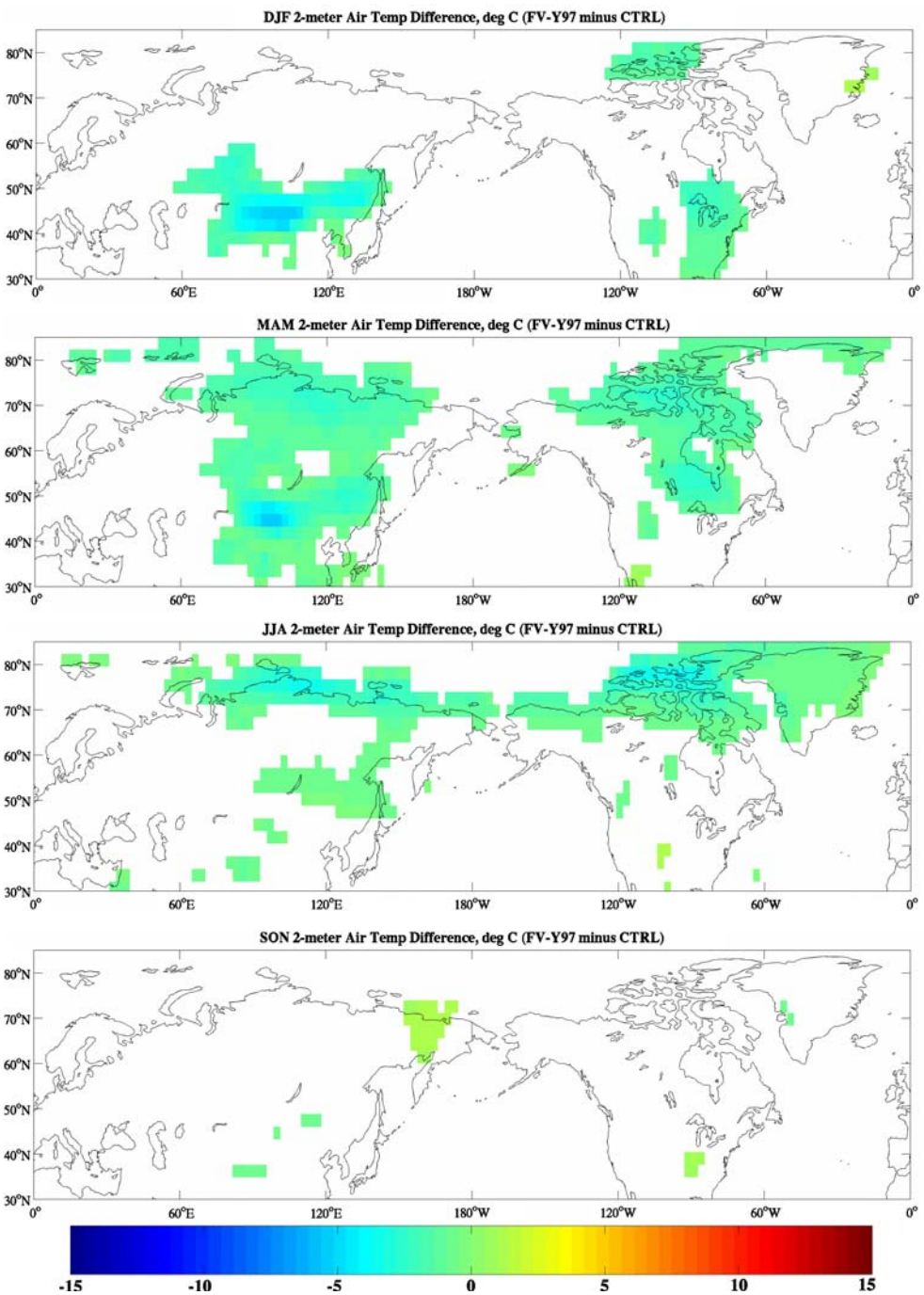


**Fig. 7** Difference in 2-m air temperature for all four seasons between the fixed vegetation case and control run (FV-Y97 minus CTRL). Insignificant differences have been masked out

that the model is relatively insensitive to the choice of snow cover parameterization. And one might justify its inclusion based on previous studies showing that it provides a better fit with snow cover and albedo observations (Yang et al. 1997). Indeed, the cooling from the increased snow cover from the Y97 algorithm is relatively minor. This slight push to the climate model, however, is enough to send the dynamic vegetation into a trajectory towards much reduced boreal vegetation, persistent snow cover over large regions throughout the year, higher surface albedos, and a much colder equilibrium climate.

How realistic is the rapid vegetation response in this model? Paleoecological records, and even some recent observational studies, point to the potential for large scale, rapid shifts in vegetation dynamics and distributions associated with climatic change. Evidence for rapid changes in vegetation composition, with timescales on the order of decades (similar to our study), have been found during

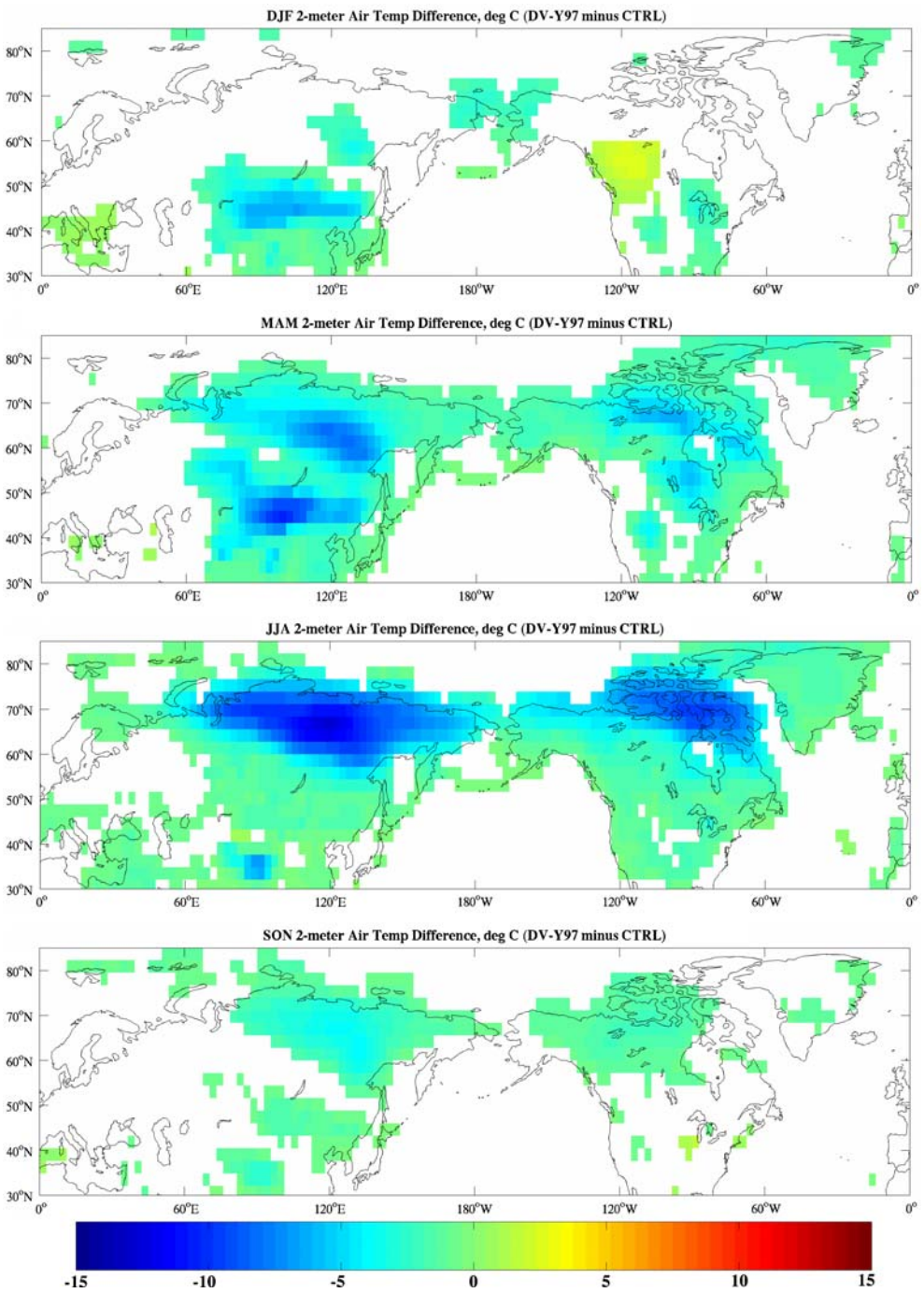


**Fig. 8** Difference in 2-m air temperature for all four seasons between the dynamic vegetation case and control run (DV-Y97 minus CTRL). Insignificant differences have been masked out

abrupt climate events like the Younger Dryas (Peteet 2000; Williams et al. 2002; Yu 2007). The fastest vegetation responses are typically observed in areas with strong vegetation gradients (ecotones), such as the coastal tundra in Alaska and mixed composition (boreal and temperate trees) forests in New England and the Appalachians (Peteet 2000). This fits well with our modeling results, which show rapid vegetation changes in the boreal region of the Northern Hemisphere, where a strong temperature gradient drives a steep gradient in vegetation (from boreal tree species to grasses). Evidence for rapid vegetation responses to climate change have been found in other regions as well, including the tropics (Hughen et al. 2004), and semiarid areas (Allen and Breshears 1998; Breshears et al. 2005). Given the evidence for rapid vegetation responses in the past, the rapid dieback of vegetation to a cold anomaly within our model is plausible. Additionally, the vegetation model used here (CLM-DGVM, based on the LPJ-DGVM)

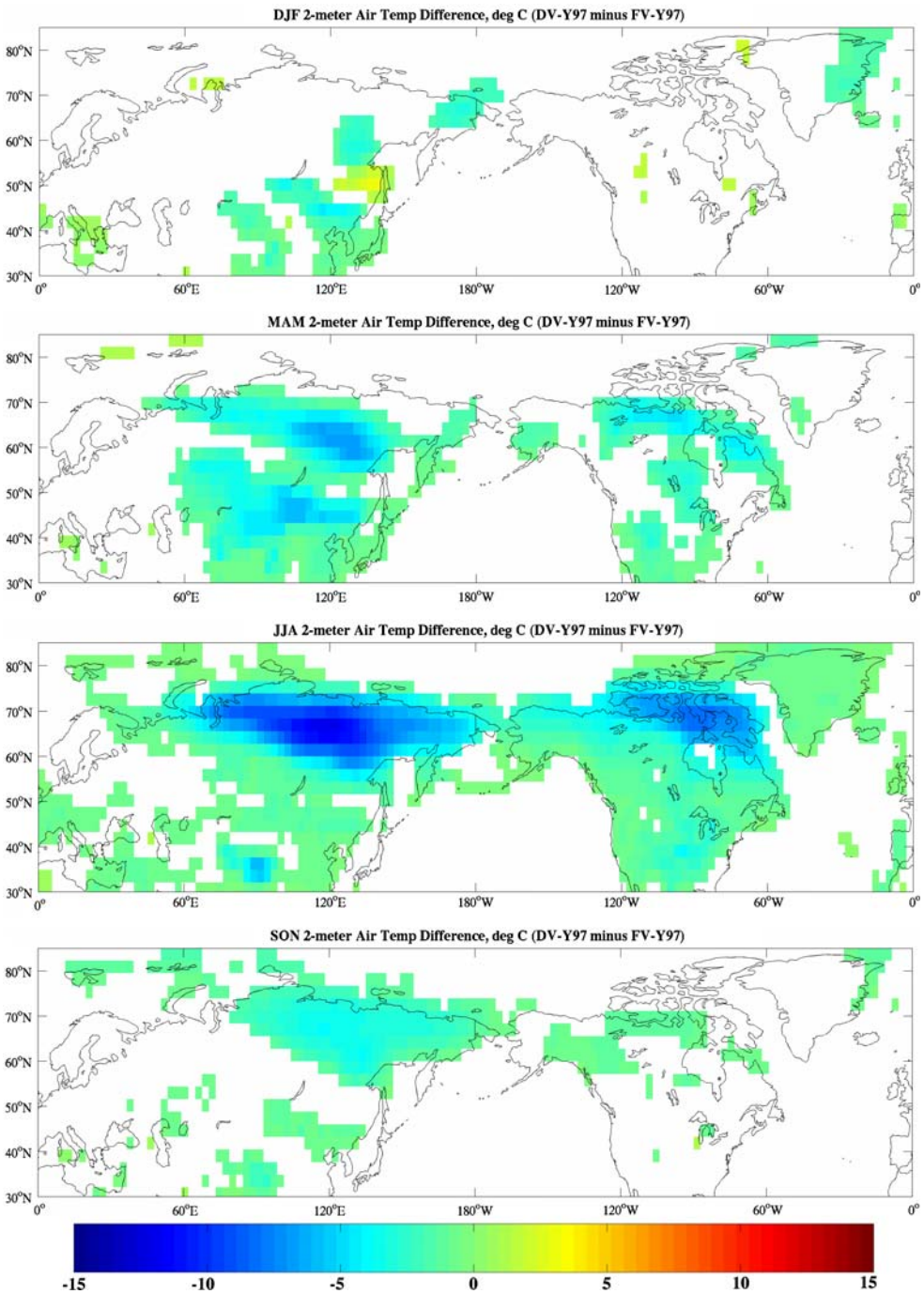


**Fig. 9** Difference in 2-m air temperature for all four seasons between the dynamic vegetation case and fixed vegetation case (DV-Y97 minus FV-Y97). Insignificant differences have been masked out

shows similar timescales for carbon and vegetation dynamics when compared to an independent vegetation model forced by the same climate scenarios (Bachelet et al. 2003). This gives some confidence that the results here are not necessarily model dependent.

The initial forcing of the vegetation within our study was from increased cold stress during the fall/winter/spring seasons, from higher land surface albedo via increased snow cover in the Y97 algorithm (Fig. 5). The vegetation response amplified this effect, further increasing cold stress and leading to an expansion of the albedo and temperature anomalies into the summer season. Vegetation, of course, can be sensitive to a variety of climatic thresholds, related to both temperature and moisture. Gallimore (2005), for example, found that increased seasonality (warmer summers/colder winters) led to the expansion of grasslands at

**Table 3** Summary of the surface energy balance (units of W $m^{-2}$) for each scenario, broken down by season and latitude band

| Flux | CTRL | FV-Y97 | DV-Y97 | Difference FV-CTRL | Difference DV-CTRL |
|---|---|---|---|---|---|
| Area average surface energy fluxes (W $m^{-2}$), DJF | | | | | |
| Latitude 60°–90° | | | | | |
| Incident solar | 7.81 | 8.13 | 8.30 | 0.32 | 0.49 |
| Absorbed solar | 3.36 | 2.90 | 2.57 | −0.46 | −0.80 |
| Reflected solar | 4.45 | 5.22 | 5.73 | 0.78 | 1.29 |
| Heat flux into ground | −10.45 | −9.96 | −8.69 | 0.49 | 1.76 |
| SH flux | 9.18 | 9.22 | 9.22 | 0.03 | 0.01 |
| LH flux | 2.15 | 2.33 | 2.05 | 0.18 | −0.10 |
| Snow melt heat flux | 0.36 | 0.39 | 0.36 | 0.03 | 0.01 |
| Latitude 30°–60° | | | | | |
| Incident solar | 78.22 | 81.68 | 82.37 | 3.45 | 4.15 |
| Absorbed solar | 57.34 | 53.68 | 52.01 | −3.66 | −5.33 |
| Reflected solar | 20.89 | 28.00 | 30.36 | 7.12 | 9.48 |
| Heat flux into ground | −10.11 | −10.30 | −10.22 | −0.20 | −0.12 |
| SH flux | 36.43 | 35.27 | 35.50 | −0.19 | −0.25 |
| LH flux | 18.52 | 17.02 | 16.25 | −1.50 | −2.27 |
| Snow melt heat flux | 1.66 | 1.47 | 1.41 | −0.19 | −0.25 |
| Area average surface energy fluxes (W $m^{-2}$), JJA | | | | | |
| Latitude 60°–90° | | | | | |
| Incident solar | 233.97 | 240.56 | 244.21 | 6.59 | 10.24 |
| Absorbed solar | 143.59 | 126.87 | 86.36 | −16.72 | −57.23 |
| Reflected solar | 90.38 | 113.69 | 157.85 | 23.32 | 67.48 |
| Heat flux into ground | 14.80 | 13.01 | 6.14 | −1.79 | −8.65 |
| SH flux | 28.35 | 25.80 | 20.61 | −2.54 | −7.74 |
| LH flux | 20.88 | 19.37 | 11.04 | −1.52 | −9.84 |
| Snow melt heat flux | 6.39 | 8.93 | 13.77 | 2.54 | 7.38 |
| Latitude 30°–60° | | | | | |
| Incident solar | 312.41 | 313.08 | 307.84 | 0.67 | −4.57 |
| Absorbed solar | 261.18 | 261.55 | 252.99 | 0.37 | −8.19 |
| Reflected solar | 51.23 | 51.53 | 54.85 | 0.30 | 3.62 |
| Heat flux into ground | 11.08 | 11.64 | 11.82 | 0.56 | 0.74 |
| SH flux | 67.29 | 65.82 | 65.44 | −1.47 | −1.85 |
| LH flux | 60.14 | 60.72 | 58.35 | 0.58 | −1.79 |
| Snow melt heat flux | 0.09 | 0.23 | 1.04 | 0.14 | 0.95 |
| Area average surface energy fluxes (W $m^{-2}$), MAM | | | | | |
| Latitude 60°–90° | | | | | |
| Incident solar | 177.27 | 186.31 | 189.02 | 9.04 | 11.75 |
| Absorbed solar | 74.44 | 65.85 | 58.66 | −8.59 | −15.78 |
| Reflected solar | 102.83 | 120.45 | 130.37 | 17.62 | 27.54 |
| Heat flux into ground | 0.55 | −0.37 | −0.74 | −0.92 | −1.29 |
| SH flux | 15.03 | 13.63 | 13.45 | −1.40 | −1.58 |
| LH flux | 14.91 | 14.13 | 12.75 | −0.78 | −2.15 |
| Snow melt heat flux | 7.43 | 5.68 | 4.50 | −1.75 | −2.93 |
| Latitude 30°–60° | | | | | |
| Incident solar | 233.83 | 237.93 | 240.03 | 4.10 | 6.20 |
| Absorbed solar | 186.78 | 182.41 | 169.39 | −4.37 | −17.39 |
| Reflected solar | 47.05 | 55.52 | 70.64 | 8.47 | 23.59 |
| Heat flux into ground | 7.41 | 6.86 | 5.26 | −0.55 | −2.15 |

**Table 3** continued

| Flux | CTRL | FV-Y97 | DV-Y97 | Difference FV-CTRL | Difference DV-CTRL |
|---|---|---|---|---|---|
| SH flux | 45.15 | 43.14 | 42.84 | −2.00 | −2.31 |
| LH flux | 43.05 | 42.32 | 38.08 | −0.73 | −4.97 |
| Snow melt heat flux | 4.63 | 4.93 | 4.98 | 0.29 | 0.35 |
| Area average surface energy fluxes (W $m^{-2}$), SON | | | | | |
| Latitude 60°–90° | | | | | |
| Incident solar | 34.28 | 35.23 | 36.62 | 0.95 | 2.34 |
| Absorbed solar | 21.71 | 19.94 | 15.69 | −1.77 | −6.02 |
| Reflected solar | 12.57 | 15.30 | 20.93 | 2.72 | 8.36 |
| Heat flux into ground | −11.98 | −10.56 | −8.54 | 1.42 | 3.44 |
| SH flux | 17.33 | 16.92 | 17.08 | −0.41 | −0.25 |
| LH flux | 9.03 | 8.32 | 8.84 | −0.71 | −0.20 |
| Snow melt heat flux | 0.79 | 0.79 | 1.06 | −0.01 | 0.27 |
| Latitude 30°–60° | | | | | |
| Incident solar | 141.10 | 141.62 | 141.28 | 0.52 | 0.18 |
| Absorbed solar | 114.88 | 114.59 | 112.82 | −0.29 | −2.06 |
| Reflected solar | 26.22 | 27.03 | 28.46 | 0.82 | 2.25 |
| Heat flux into ground | −10.60 | −10.51 | −9.84 | 0.09 | 0.76 |
| SH flux | 48.29 | 47.86 | 48.43 | −0.42 | 0.14 |
| LH flux | 24.65 | 24.92 | 24.37 | 0.27 | −0.29 |
| Snow melt heat flux | 0.60 | 0.57 | 0.59 | −0.03 | −0.01 |

the expense of forests in midlatitude continental interiors by both increasing moisture stress during the summer and increasing cold stress during the winter. In their study, warm and cold season climate changes, though of opposite sign, had a synergistic (complementary) influence on vegetation dynamics. To expand on our work, a separate set of experiments could be conducted, focused on warm season climate (e.g., by changing soil parameterizations to look at moisture stress). This may help shed some light on the relative sensitivity of vegetation to cold versus warm season climatic changes, including the potential for synergistic effects.

Finally, how would the results seen here compare to other coupled models? We have already noted that CAM3-CLM3 has some of the strongest land–atmosphere coupling compared to a suite of other current models (Guo et al. 2006; Koster et al. 2006). If this biased our results, however, we might expect a greater model response from just the FV-Y97 scenario. In fact, this implies that even models with strong land–atmosphere coupling may be relatively insensitive to certain modifications of the land surface scheme unless they are coupled to model components with longer system memory. Historically these other model components have included the oceans and sea ice, but the study here shows that dynamic vegetation can also impart enough memory into the climate system and lead to a large model response. The implication here is that dynamic vegetation, much like sea ice and dynamical ocean models, should be a crucial consideration during the development and modification of coupled climate models.

**Acknowledgments** This work was supported, in part, by National Science Foundation Grant #OPP-0531166, Greening of the Arctic. BIC acknowledges the academic and financial support of the University of Virginia, Department of Environmental Sciences and the National Center for Atmospheric Research. The National Center for Atmospheric Research is sponsored by the National Science Foundation.

## References

Allen CD, Breshears DD (1998) Drought-induced shift of a forest-woodland ecotone: rapid landscape response to climate variation. Proc Natl Acad Sci 95:14839–14842

Bachelet D, Neilson RP, Hickler T, Drapek RJ, Lenihan JM, Sykes MT, Smith B, Sitch S, Thonicke K (2003) Simulating past and future dynamics of natural ecosystems in the United States. Global Biogeochem Cycles. doi:10.1029/2001GB001508

Barnett TP, Dumenil L, Schlese U, Roeckner E, Latif M (1989) The effect of Eurasian snow cover on regional and global climate variations. J Atmos Sci 46:661–686

Bonan GB, Levis S (2006) Evaluating aspects of the community land and atmosphere models (CLM3 and CAM3) using a dynamic global vegetation model. J Clim 19:2290–2301

Bonan GB, Pollard D, Thompson SL (1992) Effects of boreal forest vegetation on global climate. Nature 359:716–718

Bonan GB, Oleson KW, Vertenstein M, Levis S, Zeng X, Dai Y, Dickinson RE, Yang ZL (2002) The land surface climatology of the community land model coupled to the NCAR community climate model. J Clim 15:3123–3149

Breshears DD, Cobb NS, Rich PM, Price KP, Allen CD, Balice RG, Romme WH, Kastens JH, Floyd ML, Belnap J, Anderson JJ, Myers OB, Meyer CW (2005) Regional vegetation die-off in response to global-change-type drought. Proc Natl Acad Sci 102:15144–15148

Brovkin V, Levis S, Loutre MF, Crucifix M, Claussen M, Ganopolski A, Kubatzki C, Petoukhov V (2003) Stability analysis of the climate–vegetation system in the northern high latitudes. Clim Change 57:119–138

Cess RD, Potter GL, Zhang MH (1991) Interpretation of snow-climate feedback as produced by 17 general circulation models. Science 253:888–892

Claussen M, Fohlmeister J, Ganopolski A, Brovkin V (2006) Vegetation dynamics amplifies precessional forcing. Geophys Res Lett 33. doi:10.1029/2006GL026111

Cohen J, Entekhabi D (1999) Eurasian snow cover variability and Northern Hemisphere climate predictibability. Geophys Res Lett 26:345–348

Collins WD, Rasch PJ, Boville BA, Hack JJ, McCaa JR, Williamson DL, Kiehl JT, Briegleb B, Bitz C, Lin SJ, Zhang M, Dai Y (2004) Description of the NCAR Community Atmosphere Model (CAM3). Technical Note NCAR/TN-464+STR, National Center for Atmospheric Research, Boulder, 226 pp

Collins WD, Rasch PJ, Boville BA, Hack JJ, McCaa JR, Williamson DL, Briegleb BP, Bitz CM, Lin SJ, Zhang M (2006) The formulation and atmospheric simulation of the Community Atmosphere Model: CAM3. J Clim 19:2144–2161

Dickinson RE, Oleson KW, Bonan GB, Hoffman F, Thornton PE, Vertenstein M, Yang ZL, Zeng X (2006) The Community Land Model and its climate statistics as a component of the Community Climate System Model. J Clim 19:2302–2324

Douville H, Royer JF, Mahfouf JF (1995) A new snow parameterization for the Meteo-France climate model. Clim Dyn 12:21–35

Fekete BM, Vorosmarty CJ, Grabs W (2000) Global composite runoff fields based on observed river discharge and simulated water balances. Available online at http://www.grdc.sr.unh.edu

Fekete BM, Vorosmarty CJ, Grabs W (2002) High-resolution fields of global runoff combining observed river discharge and simulated water balances. Global Biogeochem Cycles 16:1042. ( doi:10.1029/1999GB001254)

Foster DJ Jr, Davy RD (1988) Global snow depth climatology. USAF Environmental Technical Applications Center Technical Note USAFETAC TN-88 (006), 48 pp

Gallimore R, Jacob R, Kutzbach J (2005) Coupled atmosphere–ocean–vegetation simulations for modern and mid-Holocene climates: role of extratropical vegetation cover feedbacks. Clim Dyn 25:755–776

Ganopolski A, Kubatzki C, Claussen M, Brovkin V, Petoukhov V (1998) The influence of vegetation–atmosphere–ocean interaction on climate during the mid-Holocene. Science 280:1916–1919

Guo Z, Dirmeyer PA, Koster RD, Bonan GB, Chan E, Cox P, Gordon CT, Kanae S, Kowalczyk E, Lawrence D, Liu P, Lu C-H, Malyshev S, McAvaney B, Mitchell K, Mocko D, Oki T, Oleson KW, Pitman A, Sud YC, Taylor CM, Versegh D, Vasic R, Xue Y, Yamada T (2006) GLACE: the global land–atmosphere coupling experiment. Part II. Analysis. J Hydrometeorol 7:611–625

Hughen KA, Eglinton TI, Xu L, Makou M (2004) Abrupt tropical vegetation response to rapid climate changes. Science 304:1955–1959

Koster RD, Guo Z, Dirmeyer PA, Bonan GB, Chan E, Cox P, Davies H, Gordon CT, Kanae S, Kowalczyk E, Lawrence D, Liu P, Lu C-H, Malyshev S, McAvaney B, Mitchell K, Mocko D, Oki T, Oleson KW, Pitman A, Sud YC, Taylor CM, Verseghy D, Vasic R, Xue Y, Yamada T (2006) GLACE: the global land–atmosphere coupling experiment. Part I. Overview. J Hydrometeorol 7:590–610

Krinner G, Viovy N, Noblet-Ducoudre N, Ogee J, Polcher J, Friedlingstein P, Ciais P, Sitch S, Prentice IC (2005) A dynamic global vegetation model for studies of the coupled atmosphere–biosphere system. Global Biogeochem Cycles 19. doi:10.1029/2003GB002199

Lawrence DM, Thornton PE, Oleson KW, Bonan GB (2007) The partitioning of evapotranspiration into transpiration, soil evaporation, and canopy evaporation in a GCM: impacts on land–atmosphere interaction. J Hydrometeorol (in press)

Levis S, Foley JA, Pollard D (1999) $CO_2$, climate, and vegetation feedbacks at the Last Glacial Maximum. J Geophys Res-Atmos 104:31191–31198

Levis S, Bonan GB, Vertenstein M, Oleson KW (2004) The Community Land Model's Dynamic Global Vegetation Model (CLM-DGVM): technical description and user's guide. NCAR/TN-459+IA

Oleson KW, Dai Y, Bonan GB, Bosilovich M, Dickinson R, Dirmeyer P, Hoffman F, Houser P, Levis S, Niu GY, Thornton PE, Vertenstein M, Yang ZL, Zeng X (2004) Technical description of the Community Land Model (CLM). Technical Note NCAR/TN-461+STR, National Center for Atmospheric Research, Boulder, 173 pp

Peteet D (2000) Sensitivity and rapidity of vegetational response to abrupt climate change. Proc Natl Acad Sci 97:1359–1361

Sitch S, Smith B, Prentice C, Arneth A, Bondeau A, Cramer W, Kaplan JO, Levis S, Lucht W, Sykes MT, Thonicke K, Venevsky V (2003) Evaluation of ecosystem dynamics, plant geography and terrestrial carbon cycling in the LPJ dynamic global vegetation model. Global Change Biol 9:161–185

Williams JW, Post DM, Cwynar LC, Lotter AF, Levesque AJ (2002) Rapid and widespread vegetation responses to past climate change in the North Atlantic region. Geology 30:971–974

Willmott CJ, Matsuura K (2000) Terrestrial air temperature and precipitation: monthly and annual climatologies. Available online at http://climate.geog.udel.edu/~climate

Wohlfahrt J, Harrison SP, Braconnot P (2004) Synergistic feedbacks between ocean and vegetation on mid- and high-latitude climates during the mid-Holocene. Clim Dyn 22:223–238

Yang ZL, Dickinson RE, Robock A, Vinnikov KY (1997) Validation of the snow submodel of the biosphere–atmosphere transfer scheme with Russian snow cover and meteorological observational data. J Clim 10:353–373

Yu Z (2007) Rapid response of forested vegetation to multiple climate oscillations during the last deglaciation in the northeastern United States. Quat Res 67:297–303